gPCE Uncertainty Quantification Modeling for Bathymetric LiDAR and Earth Science

Alexandra K. Wise[1]*, Kevin W. Sacca[1], Jeffrey P. Thayer[1]

[1] Aerospace Engineering Sciences Department, University of Colorado at Boulder

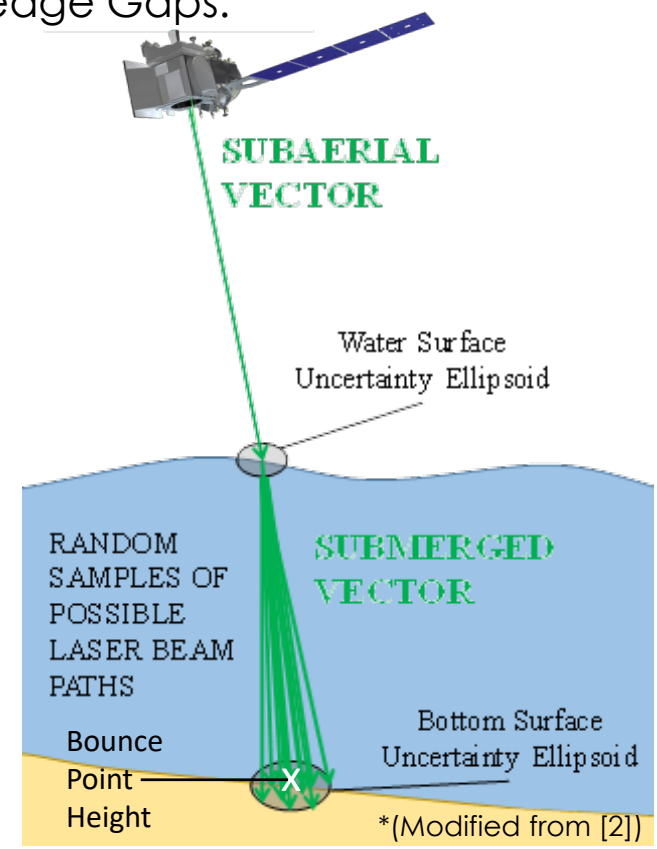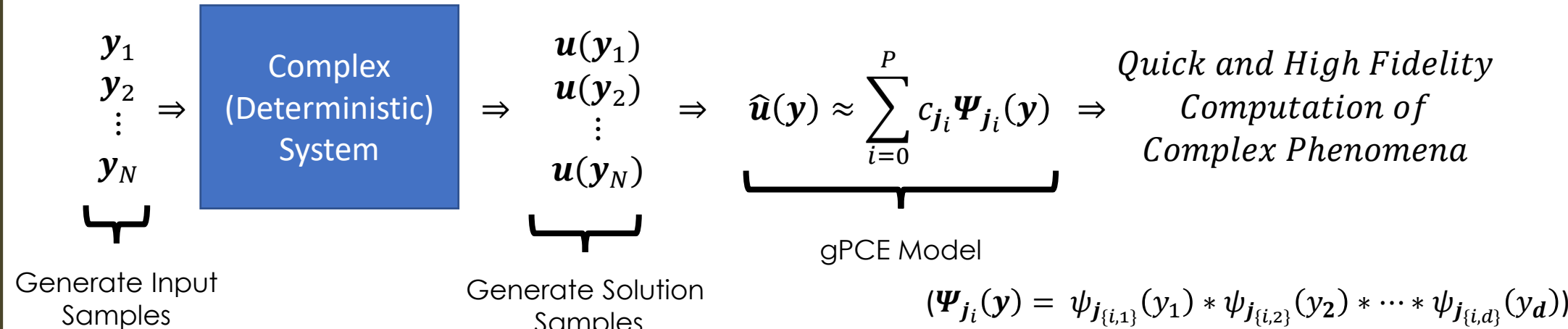*Corresponding Author: Alexandra.Wise@Colorado.edu

I. Motivation and Objectives

Motivation: Most LiDARs are vulnerable to position, pointing errors, and propagation effects leading to projection errors on target. While fidelity of location/ pointing solutions can be high, determination of uncertainty remains limited. NASA's 2021 STV Incubation Study Report lists vertical (horizontal, geolocation) accuracy as an associated product parameter for all (most) identified Science and Application Knowledge Gaps.

SUBAERIAL VECTOR

Water Surface Uncertainty Ellipsoid

RANDOM SAMPLES OF POSSIBLE LASER BEAM PATHS

SUBMERGED VECTOR

Bounce Point Height

Bottom Surface Uncertainty Ellipsoid

(Modified from [2])

Research Objectives:

- Develop gPCE method for topo-bathymetric LiDAR Uncertainty Quantification (UQ) as an alternative to Total Propagated Uncertainty (TPU) & Monte Carlo (MC) UQ methods
- Quantify & compare performance of UQ methods, in terms of computational cost & model fidelity
- Investigate subaerial simulations as validation to proceed with bathymetric simulation

II. generalized Polynomial Chaos Expansion

$$\begin{matrix} y_1 \\ y_2 \\ \vdots \\ y_N \end{matrix} \Rightarrow \text{Complex (Deterministic) System} \Rightarrow \begin{matrix} u(y_1) \\ u(y_2) \\ \vdots \\ u(y_N) \end{matrix} \Rightarrow \hat{u}(y) \approx \sum_{i=0}^{P} c_{J_i}\Psi_{J_i}(y) \Rightarrow \textit{Quick and High Fidelity Computation of Complex Phenomena}$$

Generate Input Samples → Generate Solution Samples → gPCE Model

$$(\Psi_{J_i}(y) = \psi_{J_{(i,1)}}(y_1) * \psi_{J_{(i,2)}}(y_2) * \cdots * \psi_{J_{(i,d)}}(y_d))$$

generalized Polynomial Chaos Expansion (gPCE) framework is analogous to a Fourier Series Expansion

- Truncated infinite series of coefficients & orthogonal basis functions (Karhunen-Loève Expansion)

gPCE utilizes **Askey basis functions** (see table below, right)

- **Minimized mean squared error** and **guaranteed to converge,** for smooth functions with sufficient terms

The general gPCE procedure (see figure above):

- **ICESat-2 Photon Bounce Point Geolocation Algorithm** analog is used to generate solution samples, $u(y_i)$
- Multivariate basis functions, $\Psi_{J_i}(y_i)$, evaluated, and $\Psi c = u$ inverted to solve for gPCE coefficients, c
- L2 Minimization (L2M, i.e., Ordinary Least Squares) used for inversion (see V. Future Work for details)

$$\begin{bmatrix} \Psi_0(y_1) & \cdots & \Psi_P(y_1) \\ \vdots & \ddots & \vdots \\ \Psi_0(y_N) & \cdots & \Psi_P(y_N) \end{bmatrix} \begin{Bmatrix} c_0 \\ \vdots \\ c_P \end{Bmatrix} \approx \begin{Bmatrix} u(y_1) \\ \vdots \\ u(y_N) \end{Bmatrix}$$

Nx(P+1) Measurement Matrix (P+1)x1 Coefficient Vec. Nx1 Solution Samples

y	Distribution of y	Askey Polynomial	Support
Continuous	Gaussian	Hermite	$(-\infty, +\infty)$
	Gamma	Laguerre	$(0, +\infty)$
	Beta	Jacobi	$[a, b]$
	Uniform	Legendre	$[a, b]$
Discrete	Poisson	Charlier	$\{0, 1, \cdots\}$
	Binomial	Krawtchouk	$\{0, 1 \cdots, N\}$

W. Schoutens, 2000, D. Xiu and G. Karniadakis, 2002

Uncertainty Quantification:

- Inputs, y_i, are intrinsically treated as stochastic by the gPCE method
- Modeled as $y_i = x + \omega$, with deterministic component, x, and stochastic component, ω

Novel part of approach is concurrent modelling of deterministic components

- **Allows surrogate model to be applied on the point cloud level, rather than at each lidar point.**

III. gPCE vs. TPU vs. Monte Carlo: Uncertainty Quantification (UQ) Method Comparison

TPU — (Basic) Total Propagated Uncertainty (& Solution) Method

gPCE — generalized Polynomial Chaos Expansion Method

MC — (Equivalent) Monte Carlo Uncertainty (& Solution) Method

DM is identical for all methods
Deterministic Model (DM) is used to calculate Quantity of Interest (QoI, e.g., bounce point)

All three have several steps in common.
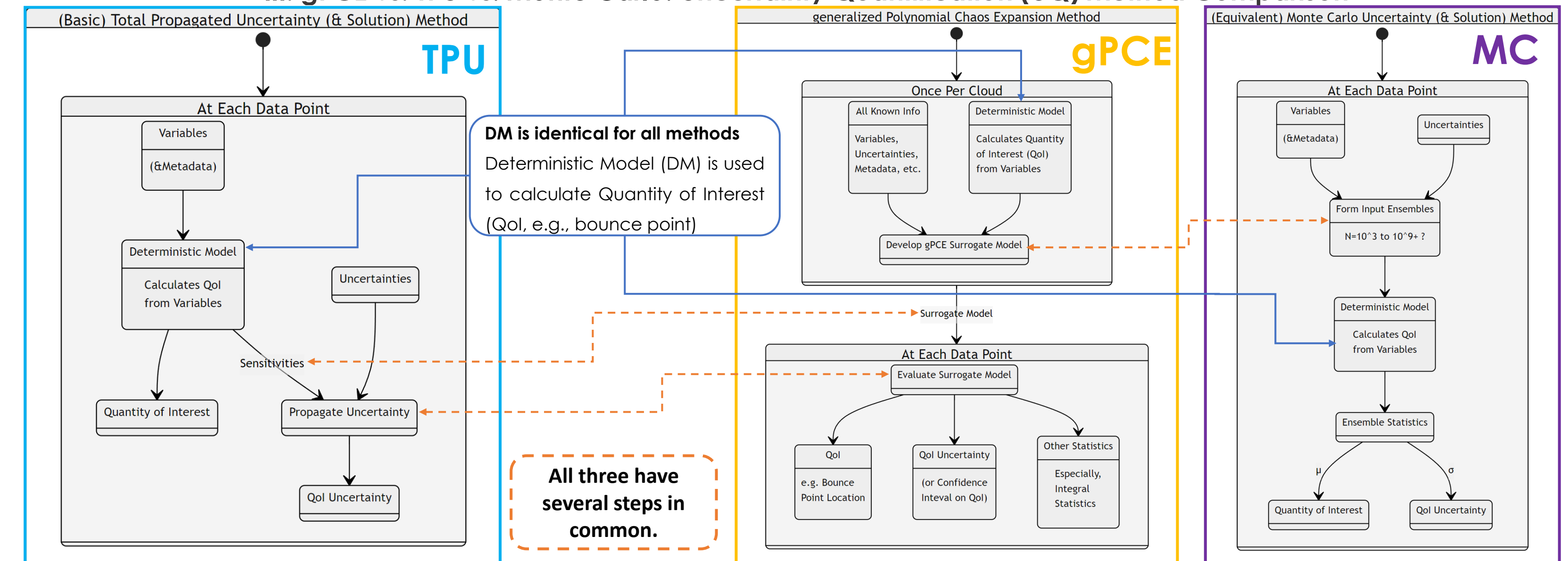
Differences are in computational time

- TPU, MC: costly steps executed once per data point/group of points (with ≅ inputs)
- gPCE: costs incurred once per point cloud (at the granule/large data segment level); Minimal computation for each point

gPCE finds high fidelity UQ models
- Cross-variable sensitivity not truncated (as a result, sensitivity studies are built-in)
- TPU often ignores/truncates these terms

Computational cost/time lies between that of TPU and MC
- (MC is prohibitively expensive for similar model per point accuracy)
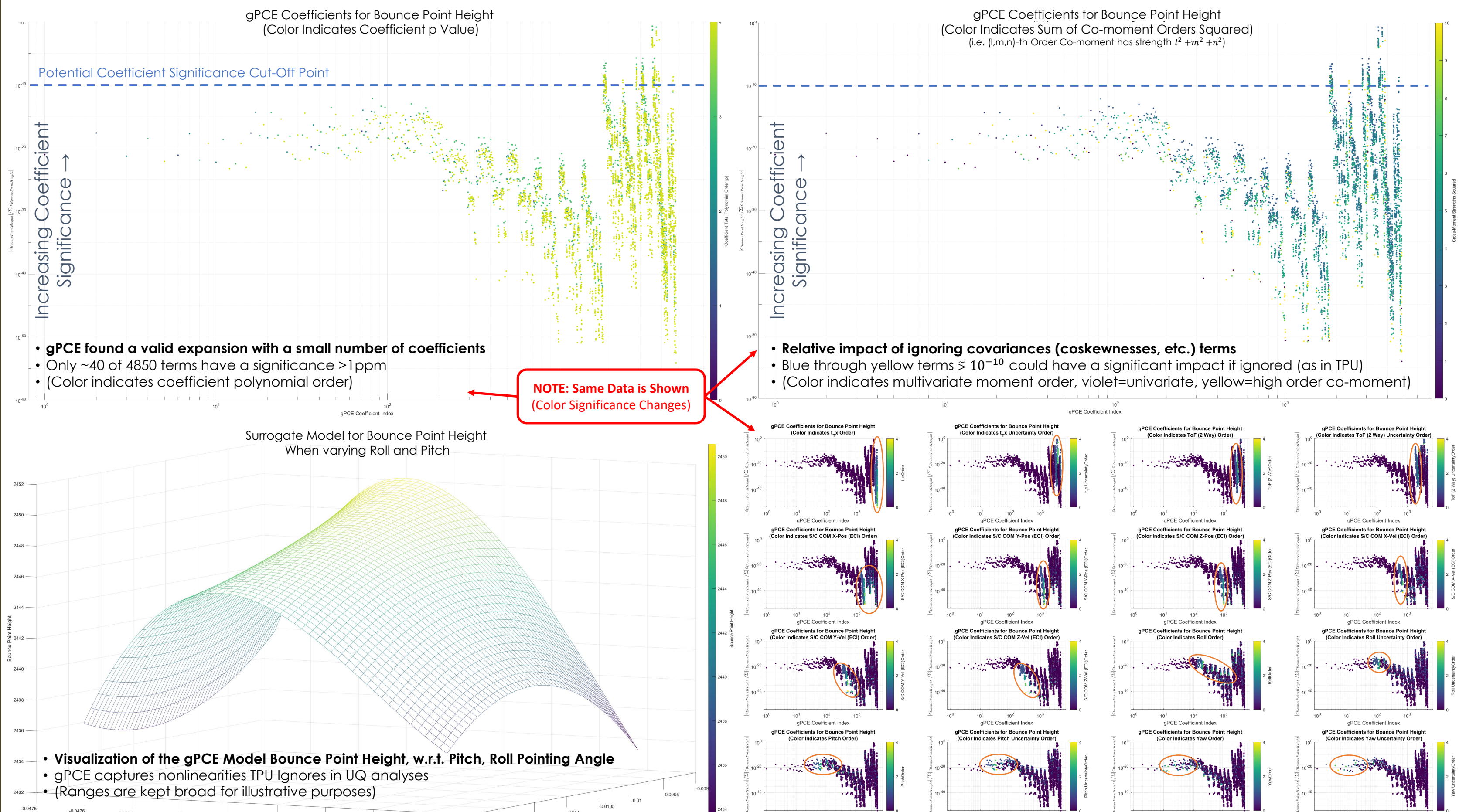
gPCE generates a joint-function/model for all input variables
- Additional statistics of interest can be found with little extra computational cost

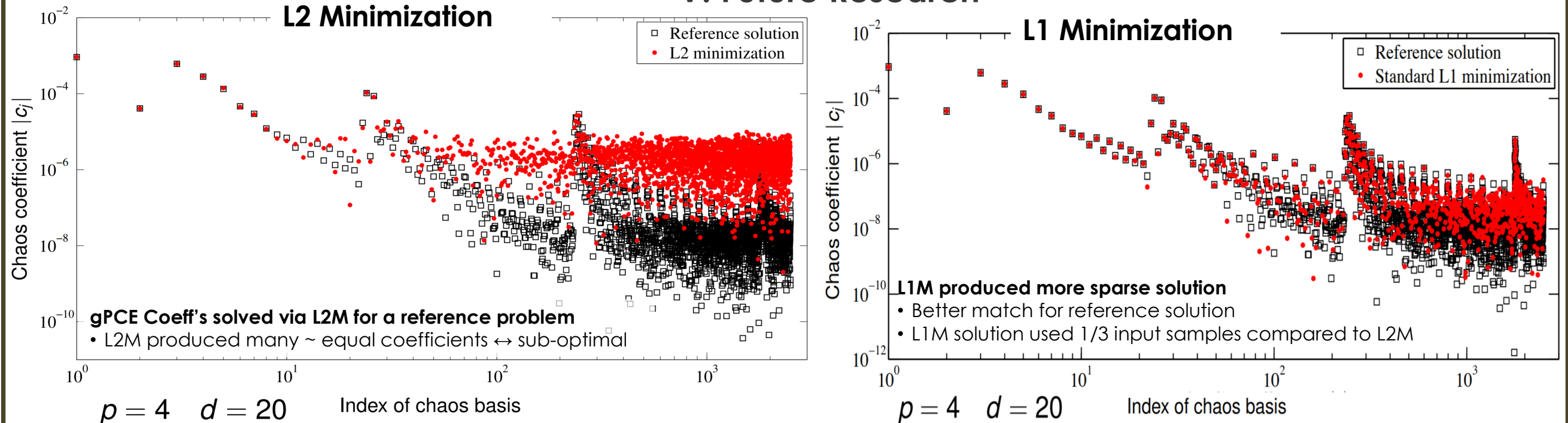| Technique	Per Point Cloud Computational Cost	Per Point Compute Cost	Model Fidelity	Additional Functionality
gPCE	High, but Feasible	Low	High	Representation of Stochastic Variables, Additional Output Statistics
TPU	Low	Low	Low	
(Equivalent) Monte Carlo	None	Prohibitively High	(Depends on Ensemble Size)	Representation of Stochastic Variables

IV. Topographic LiDAR Simulation Results

- Topographic results are presented due to instability of L2M inversion (and anticipated increased instability with Bathymetric Simulation)
- Stable bathymetric results expected with L1M inversion (see V. Future Work)

gPCE Coefficients for Bounce Point Height (Color Indicates Coefficient p Value)

Potential Coefficient Significance Cut-Off Point

Increasing Coefficient Significance →

- **gPCE found a valid expansion with a small number of coefficients**
- Only ~40 of 4850 terms have a significance >1ppm
- (Color indicates coefficient polynomial order)

gPCE Coefficients for Bounce Point Height (Color Indicates Sum of Co-moment Orders Squared) (i.e. (l,m,n)-th Order Co-moment has strength $l^2 + m^2 + n^2$)

- **Relative impact of ignoring covariances (coskewnesses, etc.) terms**
- Blue through yellow terms ≲ 10^{-10} could have a significant impact if ignored (as in TPU)
- (Color indicates multivariate moment order, violet=univariate, yellow=high order co-moment)

NOTE: Same Data is Shown (Color Significance Changes)

Surrogate Model for Bounce Point Height When varying Roll and Pitch

- **Visualization of the gPCE Model Bounce Point Height, w.r.t. Pitch, Roll Pointing Angle**
- gPCE captures nonlinearities TPU Ignores in UQ analyses
- (Ranges are kept broad for illustrative purposes)

- **gPCE Enables High Fidelity Assessment of Parameter Input-Output Relationship**
- Color indicates polynomial order of coefficients in a particular variable
- Ordinate of figures represents the relative strength ($|c_i|/\sum |c_i|$) of each coefficient.
- Higher y-position indicates greater model significance

Variables used in this simulation are from ICESat-2 ATL02, ATL03 data, and span the Region 2 granule. Surrogate Model Graph corresponds to a specific LiDAR bounce point in the mountains west of Boulder, CO, at ~40.0N, 105.4W. (NOTE: The authors recognize that Pitch, Yaw do not represent real ATLAS pointing angles; in the interest of model simplicity, Pitch, Roll, Yaw, were varied as a substitute for real pointing data, with other pointing variables held fixed.)

V. Future Research

L2 Minimization

□ Reference solution
■ L2 minimization

$p = 4$ $d = 20$ Index of chaos basis

gPCE Coeff's solved via L2M for a reference problem
- L2M produced many ~ equal coefficients ↔ sub-optimal

L1 Minimization

□ Reference solution
■ Standard L1 minimization

$p = 4$ $d = 20$ Index of chaos basis

L1M produced more sparse solution
- Better match to reference solution
- L1M solution used 1/3 input samples compared to L2M

Optimize Sparsity of Coefficient Matrix
- Computationally optimal solution is a sparse solution of large coefficients
- Replace L2 (L2M) with L1 Minimization (L1M) for coefficient inversion
- L2M: less complex, but **non-convex, NP-hard to compute,** and **non-unique results**
- L1M: shown to be a **convex, solvable in P-time, unique,** and **highly sparse** solutions (under certain conditions), requires **smaller set of input samples** (y_i)

Computational Optimizations/Improvements
- Implementation of coefficient thresholding scheme
- Implementation of entire point-cloud analysis with point uncertainty estimates
- Test actual performance of uncertainty estimates against truth data

Advance Towards a Bathymetric LiDAR model
- Verify Topographic model computationally stability and cost
- Characterize bathymetric impact on geolocation algorithm
- Use point cloud gPCE model & UQ estimates for underwater object classification
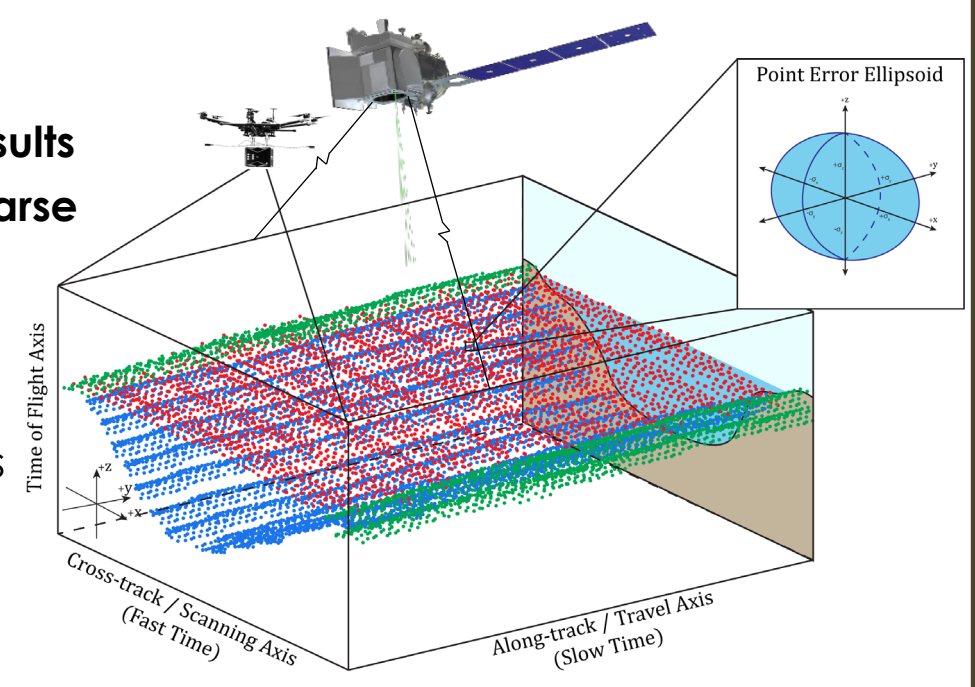
VII. References

[1] S. B. Luthcke, T. C. Thomas, T. A. Pennington, T. W. Rebold, J. B. Nicholas, D. D. Rowlands, A. S. Gardner, and S. Bae, "ICESat-2 Pointing Calibration and Geolocation Performance," Earth and Space Science, vol. 8, no. 3, pp. 1–11, 2021.
[2] F. Eren, J. Jung, C. E. Parrish, N. Sarkozi-Forfinski, and B. R. Calder, "Total vertical uncertainty (TVU) modeling for topo-bathymetric LiDAR systems," Photogrammetric Engineering and Remote Sensing, vol. 85, no. 8, pp. 585–596, 2019.
[3] T. Scott B. Luthcke, Teresa Pennington and T. Thomas, "ICESat-2 ATL03g: ATBD for ATL03g ICESat-2 Receive Photon Geolocation," tech. rep., 2019.
[4] S. Bae, J. Magruder, N. Smith, and B. Schutz, "ICESat-2 ATBD for Precision Pointing Determination," tech. rep.
[5] A. J. Martino, M. R. Bock, T. A. Neumann, D. W. H. Iii, R. L. Iii, P. W. Dabney, and C. E. Webb, "ICESat-2 ATL02: Level 1B Data Product Processing," tech. rep., 2020.
[6] T. Neumann, A. C. Brenner, D. W. Hancock, J. Robbins, J. Saba, K. Harbeck, and A. Gibbons, "ICESat-2 ATL03: ATBD for Global Geolocated Photons," tech. rep., 2021.
[7] S. Bae, M. Helgeson, M. James, L. Magruder, J. Sipps, S. Luthcke, and T. Thomas, "Performance of ICESat-2 Precision Pointing Determination," Earth and Space Science, vol. 8, no. 4, pp. 1–18, 2021.
[8] NATIONAL GEOSPATIAL-INTELLIGENCE AGENCY, "World Geodetic System 1984 (WGS84)," tech. rep., 2014.
[9] Petrov, "ICESat-2 ATL03a: ATBD for Atmospheric Delay Correction to Laser Altimetry Ranges," tech. rep., 2014.
[10] V. Coppola, J. H. Seago, and D. A. Vallado, "The IAU 2000A and IAU 2006 precession-nutation theories and their implementation," Advances in the Astronautical Sciences, vol. 134, no. January, pp. 919–938, 2009.
[11] S. B. Luthcke, N. P. Zelensky, D. D. Rowlands, F. G. Lemoine, and T. A. Williams, "The 1-centimeter orbit: Jason-1 precision orbit determination using GPS, SLR, DORIS, and altimeter data," Marine Geodesy, vol. 26, no. 3-4, pp. 399–421, 2003.
[12] S. B. Luthcke, T. Pennington, B. D. Loomis, T. Rebold, T. C. Thomas, and E. N. Gofu, "ICESat-2 ATBD for Precise Orbit Determination, Orbit Design, and Geolocation Parameter Calibration," tech. rep., 2019.
[13] T. A. Neumann, A. Brenner, D. Hancock, J. Robbins, J. Saba, K. Harbeck, A. Gibbons, J. Lee, S. B. Luthcke, T. Rebold, and E. Al., "ICESat-2 ATL03 Known Issues," Tech. Rep. January 2021, NASA, 2021.